Published in final edited form as:
Biochemistry. 2009 November 24; 48(46): 11026–11031. doi:10.1021/bi901397h.

The Human Asparaginase-Like Protein 1 hASRGL1is an Ntn Hydrolase with β-aspartyl Peptidase Activity

Jason R. Cantor[1,*], **Everett M. Stone**[1,*], **Lynne Chantranupong**, and **George Georgiou**[1,2]
[1]Department of Chemical Engineering, University of Texas, Austin, Texas 78712, USA
[2]Institute for Cell and Molecular Biology, University of Texas, Austin, Texas 78712, USA

Abstract

Herein we report the bacterial expression, purification, and enzymatic characterization of the human asparaginase-like protein 1 (hASRGL1). We present evidence that hASRGL1 exhibits β-aspartyl peptidase activity consistent with enzymes designated as plant-type asparaginases, which had thus far only been found in plants and bacteria. Similar to non-mammalian plant-type asparaginases, hASRGL1 is shown to be an Ntn hydrolase for which Thr168 serves as the essential N-terminal nucleophile for intramolecular processing and catalysis, corroborated in part by abolishment of both activities through the point-mutation Thr168Ala. In light of the activity profile reported here, ASRGL1s may act synergistically with protein L-isoaspartyl methyl transferase to relieve accumulation of potentially toxic isoaspartyl peptides in mammalian brain and other tissues.

L-asparaginases (L-asparagine amidohydrolases, EC 3.5.1.1) catalyze the hydrolysis of L-asparagine to L-aspartic acid and ammonia. Enzymes with L-asparaginase activity are classified into either the bacterial-type or plant-type subfamilies based on sequence homology, structural features, and other biochemical properties. Considerable interest has been devoted to bacterial-type asparaginases for over 40 years, in part because of their antineoplastic properties (1-4). In contrast, plant-type asparaginases have not been studied as extensively and less is known about their structural and kinetic properties. Plant-type asparaginases share a high degree of amino acid sequence similarity (60-70%) with the aspartylglucosaminidase (AGA) family (EC 3.5.1.26) (5), with both enzyme groups belonging to the N-terminal nucleophile (Ntn) hydrolase protein superfamily (6-11). Enzymes in this superfamily (12) are translated as inactive precursors which undergo an autocatalytic intramolecular activation step that exposes the N-terminal nucleophile (Thr, Ser, or Cys) at the N-terminus of the newly generated β subunit. The N-terminal nucleophile also acts as the catalytic residue during the activation step. The core folding pattern shared by Ntn-hydrolases consists of a conserved αββα structure consisting of two antiparallel β-sheets between flanking α-helical layers (13,14).

Plant-type asparaginases from plant (*Lupinus luteus* (10) and *Arabidopsis thaliana* (11)), cyanobacteria (11) (*Synechocystis sp. PCC 6803* and *Anabaena sp. PCC 7120*), and bacteria (10,11) (*E. coli*) display no hydrolytic activity towards N^4-(*β-N*-acetyl-D-glucosaminyl)-L-asparagine (GlcNAc-L-Asn), despite their high sequence similarity to AGAs. In addition to the hydrolysis of L-asparagine, they also display significant and often higher activity towards β-

Address correspondence to: George Georgiou, Ph.D., 1 University Station, C0800 Austin, Texas 78712-1084, Phone: (512) 471-6975, Fax: (512) 471-7963 gg@che.utexas.edu.
*Contributed Equally

SUPPORTING INFORMATION AVAILABLE
A table of the primers used for construction of the hASRGL1-Thr168Ala variant. This material is available free of charge via the Internet at http://pubs.acs.org.

aspartyl peptides, which has led to the suggestion that these enzymes be more accurately classified as β-aspartyl peptidases (EC 3.4.19.5) (10,11,15). Formation of isoaspartyl peptide bonds is one of the most common sources of non-enzymatic protein damage under physiological conditions, as it introduces a kink in the protein backbone that can disrupt normal folding, leading to altered susceptibility to proteolysis or loss of function (16). The β-aspartyl peptidases speculatively function to degrade these detrimental isoaspartyl peptides in the cell as they would otherwise go unnoticed by α-peptide bond specific peptidases. So far, 13 enzymes have been verified or putatively designated as β-aspartyl peptidases, but none have been identified from mammals.

A putative L-asparaginase alternatively designated asparaginase-like protein 1 (ASRGL1), Glial asparaginase (GLIAP), or CRASH (17-20), was previously cloned from rat and human cDNA libraries (17,19,20). Owing to its high sequence homology to a variety of asparaginases and AGAs, ASRGL1 was classified as an asparaginase though direct experimental evidence of its ability to turn over L-asparagine has been lacking. Herein, we describe the bacterial expression and characterization of the human ASRGL1 (hASRGL1) and demonstrate that this enzyme is an Ntn hydrolase that displays an activity profile consistent with other previously studied β-aspartyl peptidases, thus revealing hASRGL1 as the first mammalian enzyme of the β-aspartyl peptidase family.

EXPERIMENTAL PROCEDURES

Medium and Reagents

Oligonucleotides were purchased from Integrated DNA Technologies (Coralville, IA). Restriction enzymes, *Vent* DNA polymerase, T4 DNA ligase, and dNTPs were from New England Biolabs (Ipswich, MA). *o*-phthalaldehyde (OPA) reagent was from Agilent Technologies (Santa Clara, CA). Difco 2xYT growth medium was from Becton Dickinson. (Franklin Lakes, NJ) The β-aspartyl peptides, β-L-Asp-L-Phe, β-L-Asp-L-Ala, β-L-Asp-L-Leu, and β-L-Asp-L-Lys, as well as L-aspartic acid β-(7-amido-4-methylcoumarin), L-Asp β-methyl ester, and GlcNAc-L-Asn were purchased from Bachem (Torrance, CA). The β-aspartyl peptide β-L-Asp-L-Phe methyl ester was from Sigma-Aldrich (St. Louis, MO). All other reagents were from Sigma-Aldrich (St. Louis, MO) unless otherwise noted.

Molecular Biology Methods

A gene encoding the human asparaginase-like protein 1 (hASRGL1) (927 bp) with an N-terminal hexahistidine affinity tag was assembled synthetically using a set of 36 codon-optimized overlapping oligonucleotides designed by the program DNAWorks (21). *NcoI* and *EcoRI* restriction sites were incorporated into the outermost 5′ and 3′ oligonucleotides respectively. The gene assembly PCR reaction consisted of the oligonucleotide mix, ThermoPol buffer, dNTPs, and *Vent* DNA polymerase and was carried out at an initial 95°C for 2 min, followed by 30 cycles at 95°C for 1 min, 60°C for 1 min, and 72°C for 2 min, followed by a 72°C polishing step for 10 min. After a subsequent amplification reaction with the outermost oligonucleotides, the resulting DNA product was gel purified (Qiagen), digested with *NcoI/EcoRI* and ligated into pET28-a (Novagen) The gene insert in the resulting plasmid, pASRGL1, was sequenced and then ultimately transformed into *E. coli* BL21(DE3) for subsequent expression. In addition, a hASRGL1-Thr168Ala variant was constructed by overlap- extension PCR using the pASRGL1 plasmid as template and the primer pairs shown in Supplementary Table I. The point-mutant gene was cloned analogously to hASRGL1, resulting in the plasmid pASRGL1-T168A.

Expression and purification

E. coli BL21(DE3) cells containing pASRGL1 plasmid was cultured overnight at 37°C in 2xYT medium supplemented with 30 μg/mL kanamycin and used to inoculate fresh medium (1:100 dilution). When the absorbance at 600 nm (A_{600}) reached 0.5-0.7, the cells were transferred to a 25°C and allowed to equilibrate for 20 min, at which point the culture was supplemented with IPTG to a final concentration of 1 mM to induce protein expression. After 16 hr of incubation at 25°C, the cells were harvested by centrifugation at 10,000 x*g* for 10 min. The cell pellet was resuspended in binding buffer (50mM Tris-HCl, 100 mM NaCl, 10 mM imidazole, pH 8) and placed on ice. The cells were then lysed by three passes through a French pressure cell and subsequently pelleted at 40,000 x*g* for 45 min. The resulting supernatant (soluble fraction) was decanted, diluted 1:1 in binding buffer and mixed with 1 mL of pre-equilibrated nickel-nitrilotriacetic acid (Ni^{2+}-NTA) resin. After incubation for 90 min at 4°C with gentle rotation, the solution was applied to a 5 mL polypropylene column (Pierce). The resin was washed with 25 bed volumes binding buffer and 25 bed volumes wash buffer (50 mM Tris-HCl, 100 mM NaCl, 25 mM imidazole, pH 8) before the resin was incubated with 4 mL elution buffer (50 mM Tris-HCl, 100 mM NaCl, 250 mM imidazole, pH 8) for 10 min and collected drop-wise. All purification steps were performed at 4°C. The elution fraction was applied to an Amicon Ultra 10K MWCO filter, buffer exchanged against activity buffer (50 mM HEPES, 100 mM NaCl, pH 7.4), mixed with glycerol (final 10% v/v), and finally snap-frozen with liquid nitrogen and stored at −80°C. An identical protocol was followed for expression of hASRGL1-T168A. Protein concentrations were determined using a calculated extinction coefficient of 22,190 $M^{-1}cm^{-1}$(22). The expression of hASRGL1 and hASRGL1-T168A were confirmed by Western Blotting as described previously (23) using mouse monoclonal anti-polyhistidine peroxidase.

In-vitro Processing

To evaluate the autocatalytic processing of hASRGL1, aliquots of both the purified wild-type and Thr168Ala enzyme variants were incubated at 37°C (24-27) and at various times, aliquots were withdrawn and analyzed by SDS/PAGE on a 4-20% precast Tris-Glycine gel (NuSep Ltd) run under reducing conditions and stained with GelCode Blue (Thermo Scientific). To quantitatively assess the effect of 37°C incubation on intramolecular processing, gel band intensities were measured using a densitometry imaging program (Quantity 1, Bio-Rad).

Activity Assays

Catalytic activity was qualitatively determined using the fluorometric substrate L-aspartic-acid-β-7-amido-4- methylcoumarin (AspAMC). Briefly, aliquots of soluble crude cell lysate fractions were normalized to equal pre-lysis A_{600} and then diluted tenfold to 100 μL in 50 mM HEPES, 100 mM NaCl, pH 7.4. 1μL of 10 mM AspAMC in DMSO was added and mixed by pipetting in a 96 well plate (Nunc). The increase in fluorescence was monitored using a 360/40nm excitation filter and 460/40 emission filter (Synergy HT Fluorescent Platereader, BioTek) for 10 min at 25°C.

The kinetics of hASRGL1 hydrolysis were determined with freshly purified enzyme that was first incubated at 37°C for 48 hr and then stored at 4°C until needed. The formation of L-aspartic acid was determined following *o*-phthalaldehyde (OPA)- derivatization and HPLC analysis essentially as described by Agilent Technologies (28). Reactions of hASRGL1 (2-4 μM total enzyme) with substrate (concentrations from 0-5x K_M) were carried out at 37°C in 50 mM HEPES, 100 mM NaCl, pH 7.4, to a total volume of 100 μL, and were subsequently quenched with 5 μL 12% (w/v) trichloroacetic acid. An aliquot of the quenched reaction was then mixed with a molar excess (relative to substrate) of OPA reagent and brought to a final volume of 100 μL with borate buffer. The resulting solutions were analyzed by HPLC using an Agilent ZORBAX Eclipse AAA Column (C18 reverse phase, 5μm, 4.6 x 150 mm). All reactions were

done at least in triplicate and the observed rates were fit to the Michaelis-Menten equation using the program Kaleidagraph (Synergy).

RESULTS

Construction and expression of a synthetic hASRGL1 gene

The human ASRGL1 gene (GenBank accession no: BC093070) contains a number of rare *E. coli* codons such as the L-arginine codons AGA and AGG, whose presence has been shown to be detrimental to the expression of several recombinant proteins (29). To circumvent expression problems due to rare codons, a synthetic hASRGL1 fused to a 5′ sequence encoding a His_6 affinity tag was constructed by PCR gene assembly using codon-optimized oligonucleotides. The optimized hASRGL1 gene was expressed in *E. coli* BL21(DE3) and protein synthesis was confirmed by Western blot analysis with an anti-His tag antibody (Figure 1). A protein band of the expected M.W. for the full-length protein (~33 kDa) was detected in both the soluble and insoluble fractions. In addition, a lower M.W. band (~18 kDa) was observed in the soluble fraction of the wild-type enzyme only. Activity assays using the fluorometric substrate AspAMC indicated the presence of L-asparagine hydrolytic activity in cells expressing hASRGL1, but not in cells expressing hASRGL1-T168A (data not shown).

In Vitro Processing

hASRGL1 purification by immobilized metal ion affinity chromatography (IMAC) yielded 30 mg/L of protein with a purity > 90% as determined by SDS/PAGE. Incubation of purified wild-type enzyme at 37°C over time resulted in a gradual decrease of intensity in the band observed at ~33 kDa concomitant with an increase of intensity in the bands observed at ~18 kDa and ~15 kDa suggesting either specific proteolysis or intramolecular processing (Figure 2). Amino acid sequence alignment with other characterized β-aspartyl peptidases (Figure 3) identified Thr168 as the putative hASRGL1 N-terminal nucleophile requisite for the intramolecular processing characteristic of Ntn hydrolases. Consistent with this hypothesis, the hASRGL1-T168A variant was not processed to the lower M.W. bands as seen in both crude cell lysate and purified enzyme samples (Figures 1, 2). Approximately equivalent intensities of precursor and processed subunit gel bands were observed following incubation of hASRGL1 at 37°C for 48 hr, however; longer incubation times did not further enhance processing. Similarly, the rate of AspAMC hydrolysis by hASRGL1 increased over time following incubation of the enzyme at 37°C up to 48 hr, but the rate did not increase appreciably at later times (Figure 4).

The mass spectrum of the protein incubated at 37°C for 48 hr contained three prominent peaks of molecular masses 33,023 ± 11, 14547 ± 5 , and 18495 ± 6 Da corresponding to the predicted M.W.s of the precursor enzyme minus the N-terminal methionine residue (33,023 Da) and the α (expected mass 18,499 Da) and β (expected mass 14,551Da) subunits likely to be generated following intramolecular processing of the precursor at Thr168 cleavage site.

Kinetic Analysis

We determined the kinetic parameters of hydrolysis against a variety of potential hASRGL1 substrates including L-Asn; the β-aspartyl dipeptides: β-L-Asp-L-Phe, β-L-Asp-L-Phe-methyl ester, β-L-Asp-L-Ala, β-L-Asp-L-Leu, and β-L-Asp-L-Lys; L-Asp-β-methyl ester, and GlcNAc-L-Asn (Table 1). The calculation of k_{cat} was based on the observation that 50% of the total enzyme used in a given reaction was in the processed active form based on gel densitometry analysis.

The activity profile of hASRGL1 was observed to be very similar to that of enzymes designated as isoaspartyl aminopeptidases with secondary L-asparaginase activity (10,11) – classified as the β-aspartyl peptidase family (EC 3.4.19.5). The set of characterized enzymes in this family display a millimolar K_M for L-asparagine, but a lower K_M for a variety of isoaspartyl dipeptides.

Moreover, these enzymes are unable to hydrolyze GlcNAc-L-Asn and L-Gln, consistent with the results seen for hASRGL1. In contrast, bacterial type II L-asparaginases such as the well studied enzymes from *E. coli* and *Erwinia chrysanthemi*, possess a micromolar affinity for L-asparagine and relatively little to no activity towards β-aspartyl peptides (11,30). In addition, hASRGL1 was able to hydrolyze L-Asp β-methyl ester with a specificity constant greater than those for all other substrates tested.

DISCUSSION

The biochemical and structural features of plant-type asparaginases have only begun to be elucidated over the last decade. Many of these enzymes have been shown, or strongly suggested, to belong to the N-terminal nucleophile (Ntn) hydrolase superfamily (10,11). ASRGL1 has been cloned from both rat and human cDNA libraries (17,19,20), and on account of its high sequence homology to a variety of asparaginases and AGAs, it was classified as an L-asparaginase, though direct experimental evidence of its ability to hydrolyze L-asparagine had not been demonstrated. Previously, ASRGL1 was shown to be concentrated in the cytosol and abundantly expressed in the brain, testis, and liver (19,20).

Western blot, mass spectrometry and mutagenesis analyses revealed that, as its sequence homology to plant-type asparaginases implicated, hASRGL1 belongs to the Ntn hydrolase family for which Thr168 serves as the critical residue for intramolecular processing and catalytic activity. Kinetic analysis revealed that the enzyme displays both L-asparaginase and β-aspartyl peptidase activities, however, fails to hydrolyze either L-Gln or GlcNAc-L-Asn, consistent with other characterized plant-type asparaginases (10,11). The k_{cat}/K_M values for β-aspartyl peptides containing a hydrophobic amino acid were to 2-4-fold higher relative to L-Asn, whereas substitution of a basic amino acid into the β-aspartyl position resulted in a 2-fold reduction in k_{cat}/K_M, again relative to L-Asn. We also found that an L-Asp β-methyl ester is hydrolyzed by this enzyme with a k_{cat}/K_M an order of magnitude higher than that for L-Asn, possibly because the methyl-ester is a superior leaving group relative to the ammonia of L-Asn. Further, we found that the K_M value for β -L-Asp -L-Phe methyl ester (aspartame) was 4-fold higher relative to that for β-L-Asp-L-Phe, suggesting the enzyme prefers β-aspartyl dipeptides relative to longer β-aspartyl peptides, which may be related to the fact that such dipeptides are released following digestion of peptides containing a β-aspartyl linkage by certain carboxypeptidases (31). Given that the k_{cat}/K_M values for all the β-aspartyl dipeptides assayed were within 8-fold of each other, it appears reasonable to suggest that hASRGL1 is a general β-aspartyl dipeptidase, though it is possible that the optimal substrate for this enzyme has not yet been identified.

The human lysosomal AGA is the only other known mammalian enzyme for which β-aspartyl peptidase activity had been previously observed (32), however; the reported k_{cat}/K_M values of AGA for a variety of such substrates are much lower relative to those for hASRGL1.

In contrast of course, AGA displays activity towards GlcNAc-L-Asn unlike hASRGL1 and other β-aspartyl peptidases. This difference in catalytic specificity is likely a result of the divergence within the active site residues located near the L-asparagine side chain moiety (11,20) A model of the hASRGL1 structure based on E. coli isoaspartyl aminopeptidase/L-asparaginase was created from Phyre (33) and aligned to human AGA (PDB: 1APZ; with bound L-aspartate) using PyMol (34). (Figure 5). Thus, while a near exact superimposition is observed in residues that bind the common L-aspartyl terminus of the substrate, differences are apparent in residues near the product side chain. In this region, whereas hASRGL1 predominantly contains Gly residues, human AGA contains Trp34 and Phe301 which are crucial for the binding of a sugar moiety.

The physiological function of β-aspartyl peptidases from plant, cyanobacteria, and bacteria has been speculated to be related to the hydrolysis of isoaspartyl peptides (10,11). Formation of isoaspartyl peptide bonds is one of the most common sources of non-enzymatic protein damage under physiological conditions, as it introduces a kink in the protein backbone that can disrupt normal folding, leading to altered susceptibility to proteolysis, loss of function, or potential to elicit autoimmunity (16). Interestingly, the enzyme Protein L-isoaspartyl Methyltransferase (PIMT, EC 2.1.1.77) was found to have a high degree of specificity for L-isoaspartyl residues (35,36). PIMT catalyzes the S-adenosyl-L-methionine (AdoMet)-dependent methylation of the α-carboxyl of an L-isoaspartyl site. Enzymatic methylation is followed by spontaneous ester hydrolysis ultimately resulting in a mixture of isoaspartyl (~70%) and aspartyl (~30%) linkages. This isoaspartyl product can then re-enter the methylation/demethylation cycle so that eventually there is a predominant shift towards the aspartyl linkage product (16). The action of PIMT has fostered the idea that the enzyme serves an important intracellular repair function to keep isoaspartyl levels low. However, the methyltransferase activity is highly influenced by both the local sequence and solution environment around the isoaspartyl modification (37,38) and thus in some cases, a PIMT-catalyzed isoaspartyl repair cannot take place. Presumably, in these situations, the isoaspartyl-containing proteins must be degraded, though the proteolytic quality control machinery is comprised of α-peptide bond proteases. Therefore, elimination of the remaining β-aspartyl peptides may be carried out by specialized isoaspartyl peptidases – the previously postulated role for plant-type asparaginases (10).

Though PIMT is present in all mammalian tissues examined to date, levels of the enzyme are notably higher in the brain and testis similar to the distribution of hASRGL1 (19,20,39). While PIMT has been proposed to be important for the repair of damaged proteins within mature spermatozoa in the testes, its activity in the brain has proven to be crucial through the investigation of PIMT-deficient mice, which demonstrated the link between isoaspartate accumulation and neurological abnormalities (40-42). Mammalian β-aspartyl peptidases may play a synergistic role with PIMT in these particular tissues, which perhaps possess a critical need for the repair and/or degradation of isoaspartyl-damaged proteins. Furthermore, evidence for the existence of mammalian β-aspartyl peptidases may corroborate a proposed mechanism through which such enzymes could account for the steady state level of isoaspartyl-damaged proteins observed in PIMT-deficient mice despite the continuous and spontaneous generation of such proteins (43).

Supplementary Material

Refer to Web version on PubMed Central for supplementary material.

Acknowledgments

The authors thank Dr. Brent Iverson for useful discussions. This work was supported by the NIH (CA 139059) and Texas Institute for Drug and Diagnostic Development (TI3D). J.R.C also acknowledges the U.S. Department of Homeland Security (DHS) for a Graduate Fellowship under the DHS Scholarship and Fellowship Program. L.C. was supported by a fellowship from the Arnold & Mabel Beckman Foundation.

ABBREVIATIONS

AGA, aspartylglucosaminidase; Ntn, N-terminal nucleophile; GlcNAc-Asn, N^4-(*β*-*N*-acetyl-D-glucosaminyl)-L-asparagine; ASRGL1, asparaginase-like protein 1; GLIAP, glial asparaginase; OPA, *o*-phthalaldehyde; AspAMC, L-aspartic-acid-β-7-amido-4-methylcoumarin; PIMT, Protein L-isoaspartyl Methyltransferase; AdoMet, S-adenosyl-L-methionine.

REFERENCES

1. Wade HE, Elsworth R, Herbert D, Keppie J, Sargeant K. A new Lasparaginase with antitumour activity? Lancet 1968;2:776–777. [PubMed: 4175572]
2. Broome JD. Evidence that the L-asparaginase of guinea pig serum is responsible for its antilymphoma effects. II. Lymphoma 6C3HED cells cultured in a medium devoid of Lasparagine lose their susceptibility to the effects of guinea pig serum in vivo. J Exp Med 1963;118:121–148. [PubMed: 14015822]
3. Broome JD. Evidence that the L-asparaginase Activity of Guinea Pig Serum is responsible for its Antilymphoma Effects. Nature 1961;191:1114–1115.
4. Distasio JA, Niederman RA, Kafkewitz D, Goodman D. Purification and characterization of L-asparaginase with anti-lymphoma activity from Vibrio succinogenes. J Biol Chem 1976;251:6929–6933. [PubMed: 11211]
5. Michalska K, Jaskolski M. Structural aspects of L-asparaginases, their friends and relations. Acta Biochim Pol 2006;53:627–640. [PubMed: 17143335]
6. Oinonen C, Tikkanen R, Rouvinen J, Peltonen L. Three-dimensional structure of human lysosomal aspartylglucosaminidase. Nat Struct Biol 1995;2:1102–1108. [PubMed: 8846222]
7. Guo HC, Xu Q, Buckley D, Guan C. Crystal structures of Flavobacterium glycosylasparaginase. An N-terminal nucleophile hydrolase activated by intramolecular proteolysis. J Biol Chem 1998;273:20205–20212. [PubMed: 9685368]
8. Xuan J, Tarentino AL, Grimwood BG, Plummer TH Jr. Cui T, Guan C, Van Roey P. Crystal structure of glycosylasparaginase from Flavobacterium meningosepticum. Protein Sci 1998;7:774–781. [PubMed: 9541410]
9. Guan C, Liu Y, Shao Y, Cui T, Liao W, Ewel A, Whitaker R, Paulus H. Characterization and functional analysis of the cis-autoproteolysis active center of glycosylasparaginase. J Biol Chem 1998;273:9695–9702. [PubMed: 9545304]
10. Borek D, Michalska K, Brzezinski K, Kisiel A, Podkowinski J, Bonthron DT, Krowarsch D, Otlewski J, Jaskolski M. Expression, purification and catalytic activity of Lupinus luteus asparagine ß-amidohydrolase and its Escherichia coli homolog. European Journal of Biochemistry 2004;271:3215–3226. [PubMed: 15265041]
11. Hejazi M, Piotukh K, Mattow J, Deutzmann R, Volkmer-Engert R, Lockau W. Isoaspartyl dipeptidase activity of plant-type asparaginases. Biochem J 2002;364:129–136. [PubMed: 11988085]
12. Brannigan JA, Dodson G, Duggleby HJ, Moody PC, Smith JL, Tomchick DR, Murzin AG. A protein catalytic framework with an N-terminal nucleophile is capable of self-activation. Nature 1995;378:416–419. [PubMed: 7477383]
13. Saarela J, Oinonen C, Jalanko A, Rouvinen J, Peltonen L. Autoproteolytic activation of human aspartylglucosaminidase. Biochem J 2004;378:363–371. [PubMed: 14616088]
14. Michalska K, Hernandez-Santoyo A, Jaskolski M. The mechanism of autocatalytic activation of plant-type L-asparaginases. J Biol Chem 2008;283:13388–13397. [PubMed: 18334484]
15. Larsen RA, Knox TM, Miller CG. Aspartic peptide hydrolases in Salmonella enterica serovar typhimurium. J Bacteriol 2001;183:3089–3097. [PubMed: 11325937]
16. Aswad DW, Paranandi MV, Schurter BT. Isoaspartate in peptides and proteins: formation, significance, and analysis. J Pharm Biomed Anal 2000;21:1129–1136. [PubMed: 10708396]
17. Evtimova V, Zeillinger R, Kaul S, Weidle UH. Identification of CRASH, a gene deregulated in gynecological tumors. Int J Oncol 2004;24:33–41. [PubMed: 14654938]
18. Weidle UH, Evtimova V, Alberti S, Guerra E, Fersis N, Kaul S. Cell growth stimulation by CRASH, an asparaginase-like protein overexpressed in human tumors and metastatic breast cancers. Anticancer Res 2009;29:951–963. [PubMed: 19414332]
19. Dieterich DC, Landwehr M, Reissner C, Smalla KH, Richter K, Wolf G, Bockers TM, Gundelfinger ED, Kreutz MR. Gliap--a novel untypical L-asparaginase localized to rat brain astrocytes. J Neurochem 2003;85:1117–1125. [PubMed: 12753071]
20. Bush LA, Herr JC, Wolkowicz M, Sherman NE, Shore A, Flickinger CJ. A novel asparaginase-like protein is a sperm autoantigen in rats. Mol Reprod Dev 2002;62:233–247. [PubMed: 11984834]

21. Hoover DM, Lubkowski J. DNAWorks: an automated method for designing oligonucleotides for PCR-based gene synthesis. Nucleic Acids Res 2002;30:e43. [PubMed: 12000848]
22. Gill SC, von Hippel PH. Calculation of protein extinction coefficients from amino acid sequence data. Anal Biochem 1989;182:319–326. [PubMed: 2610349]
23. Griswold KE, Mahmood NA, Iverson BL, Georgiou G. Effects of codon usage versus putative 5′-mRNA structure on the expression of Fusarium solani cutinase in the Escherichia coli cytoplasm. Protein Expr Purif 2003;27:134–142. [PubMed: 12509995]
24. Shtraizent N, Eliyahu E, Park JH, He X, Shalgi R, Schuchman EH. Autoproteolytic cleavage and activation of human acid ceramidase. J Biol Chem 2008;283:11253–11259. [PubMed: 18281275]
25. Suzuki H, Kumagai H. Autocatalytic processing of gamma-glutamyltranspeptidase. J Biol Chem 2002;277:43536–43543. [PubMed: 12207027]
26. Boanca G, Sand A, Barycki JJ. Uncoupling the enzymatic and autoprocessing activities of Helicobacter pylori gamma-glutamyltranspeptidase. J Biol Chem 2006;281:19029–19037. [PubMed: 16672227]
27. Boanca G, Sand A, Okada T, Suzuki H, Kumagai H, Fukuyama K, Barycki JJ. Autoprocessing of Helicobacter pylori gamma-glutamyltranspeptidase leads to the formation of a threonine-threonine catalytic dyad. J Biol Chem 2007;282:534–541. [PubMed: 17107958]
28. http://www.chem.agilent.com/Library/datasheets/Public/5980-3088.pdf
29. Kane JF. Effects of rare codon clusters on high-level expression of heterologous proteins in Escherichia coli. Curr Opin Biotechnol 1995;6:494–500. [PubMed: 7579660]
30. Kelo E, Noronkoski T, Stoineva IB, Petkov DD, Mononen I. Beta-aspartylpeptides as substrates of L-asparaginases from Escherichia coli and Erwinia chrysanthemi. FEBS Lett 2002;528:130–132. [PubMed: 12297292]
31. Johnson BA, Aswad DW. Fragmentation of isoaspartyl peptides and proteins by carboxypeptidase Y: release of isoaspartyl dipeptides as a result of internal and external cleavage. Biochemistry 1990;29:4373–4380. [PubMed: 2140948]
32. Noronkoski T, Stoineva IB, Ivanov IP, Petkov DD, Mononen I. Glycosylasparaginase-catalyzed synthesis and hydrolysis of beta-aspartyl peptides. J Biol Chem 1998;273:26295–26297. [PubMed: 9756857]
33. Kelley LA, Sternberg MJ. Protein structure prediction on the Web: a case study using the Phyre server. Nat Protoc 2009;4:363–371. [PubMed: 19247286]
34. Delano, DW. The PyMol Graphics System. Delano Scientific, Palo Alto; CA, USA: 2002.
35. Aswad DW. Stoichiometric methylation of porcine adrenocorticotropin by protein carboxyl methyltransferase requires deamidation of asparagine 25. Evidence for methylation at the alpha-carboxyl group of atypical L-isoaspartyl residues. J Biol Chem 1984;259:10714–10721. [PubMed: 6088513]
36. O'Connor CM, Aswad DW, Clarke S. Mammalian brain and erythrocyte carboxyl methyltransferases are similar enzymes that recognize both D-aspartyl and L-isoaspartyl residues in structurally altered protein substrates. Proc Natl Acad Sci U S A 1984;81:7757–7761. [PubMed: 6595658]
37. Lowenson JD, Clarke S. Identification of isoaspartyl-containing sequences in peptides and proteins that are usually poor substrates for the class II protein carboxyl methyltransferase. J Biol Chem 1990;265:3106–3110. [PubMed: 2303443]
38. Lowenson JD, Clarke S. Structural elements affecting the recognition of Lisoaspartyl residues by the L-isoaspartyl/D-aspartyl protein methyltransferase. Implications for the repair hypothesis. J Biol Chem 1991;266:19396–19406. [PubMed: 1833402]
39. Reissner KJ, Aswad DW. Deamidation and isoaspartate formation in proteins: unwanted alterations or surreptitious signals? Cell Mol Life Sci 2003;60:1281–1295. [PubMed: 12943218]
40. Reissner KJ, Paranandi MV, Luc TM, Doyle HA, Mamula MJ, Lowenson JD, Aswad DW. Synapsin I is a major endogenous substrate for protein L-isoaspartyl methyltransferase in mammalian brain. J Biol Chem 2006;281:8389–8398. [PubMed: 16443604]
41. Kim E, Lowenson JD, Clarke S, Young SG. Phenotypic analysis of seizure-prone mice lacking L-isoaspartate (D-aspartate) O-methyltransferase. J Biol Chem 1999;274:20671–20678. [PubMed: 10400700]

42. Ikegaya Y, Yamada M, Fukuda T, Kuroyanagi H, Shirasawa T, Nishiyama N. Aberrant synaptic transmission in the hippocampal CA3 region and cognitive deterioration in protein-repair enzyme-deficient mice. Hippocampus 2001;11:287–298. [PubMed: 11769310]

43. Lowenson JD, Kim E, Young SG, Clarke S. Limited accumulation of damaged proteins in l-isoaspartyl (D-aspartyl) O-methyltransferase-deficient mice. J Biol Chem 2001;276:20695–20702. [PubMed: 11279164]

44. Larkin MA, Blackshields G, Brown NP, Chenna R, McGettigan PA, McWilliam H, Valentin F, Wallace IM, Wilm A, Lopez R, Thompson JD, Gibson TJ, Higgins DG. Clustal W and Clustal X version 2.0. Bioinformatics 2007;23:2947–2948. [PubMed: 17846036]

45. Waterhouse AM, Procter JB, Martin DM, Clamp M, Barton GJ. Jalview Version 2--a multiple sequence alignment editor and analysis workbench. Bioinformatics 2009;25:1189–1191. [PubMed: 19151095]

Fig 1.

Western blot analysis of BL21(DE3) cells expressing human ASRGL1 (hASRGL1) or hASRGL1-T168A. Samples corresponding to an equal number of cells were loaded in each lane. *S*, soluble whole cell lysate fraction; *I*, insoluble whole cell lysate fraction.

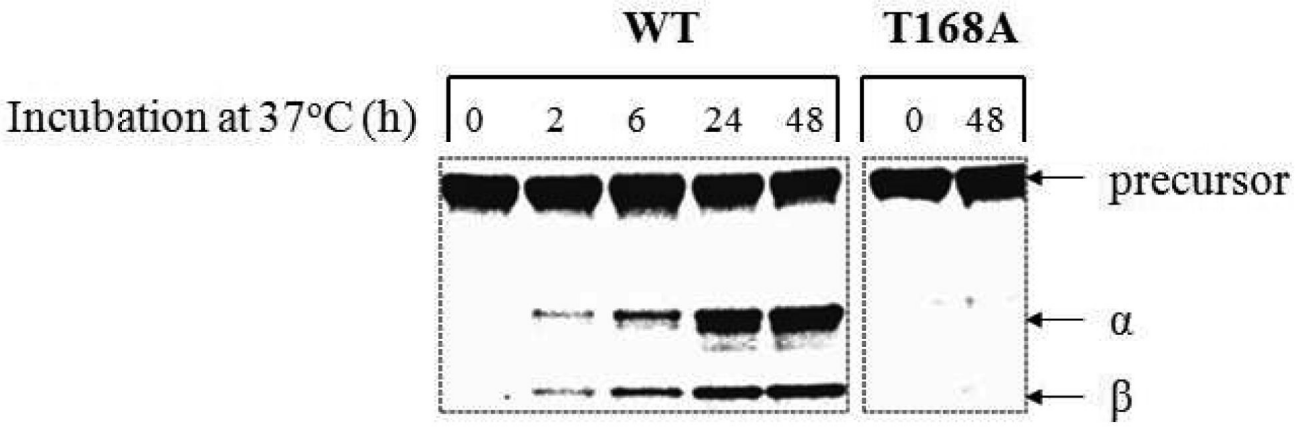

Fig 2.

SDS-PAGE of human ASRGL1 (hASRGL1) and its Thr168Ala point mutant (hASRGL1-T168A) following *in vitro* incubation at 37°C over time. Samples corresponding to an equivalent mass of total enzyme were loaded in each lane.

Fig 3.

Sequence alignment of human asparaginase-like protein 1 (hASRGL1) with plant-type asparaginases generated using ClustalW2 (*44*) and JalView (*45*) . The asterisk indicates the conserved autoproteolytic cleavage site and corresponds to residue Thr168 for the hASRGL1 sequence. Residue conservation across the alignment is denoted by the degree of shading. The sequences of the plant-type asparaginases correspond to the following UniProtKB numbers: *E. coli* (P37595); *L. Luteus* (Q9ZSD6); *Ana.7120* (Q8YQB1); *Syn.6803* (P74383).

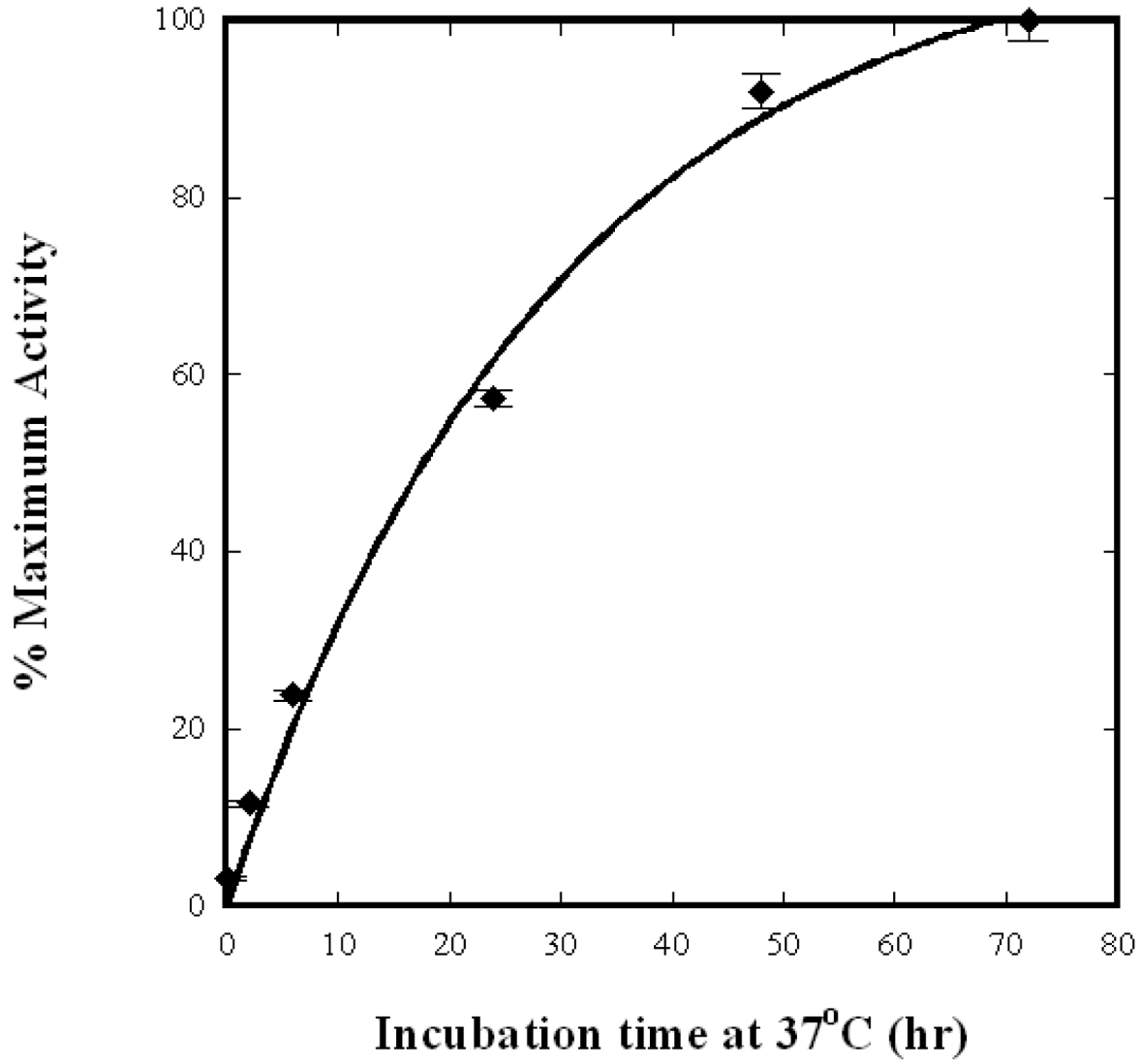

Fig 4.

Progression of intramolecular processing of human ASRGL1 (hASRGL1) following *in vitro* incubation at 37°C as determined by relative AspAMC hydrolysis rate over time. At various time points, equivalent aliquots of enzyme were withdrawn and analyzed using the fluorometric AspAMC activity assay as described under "Experimental Procedures" with the final time point serving as the maximum rate observed. The intramolecular processing reaction as evaluated through this approach exhibited $t_{1/2}$ = 20 ± 3h to maximum level of observed *in vitro* processing.

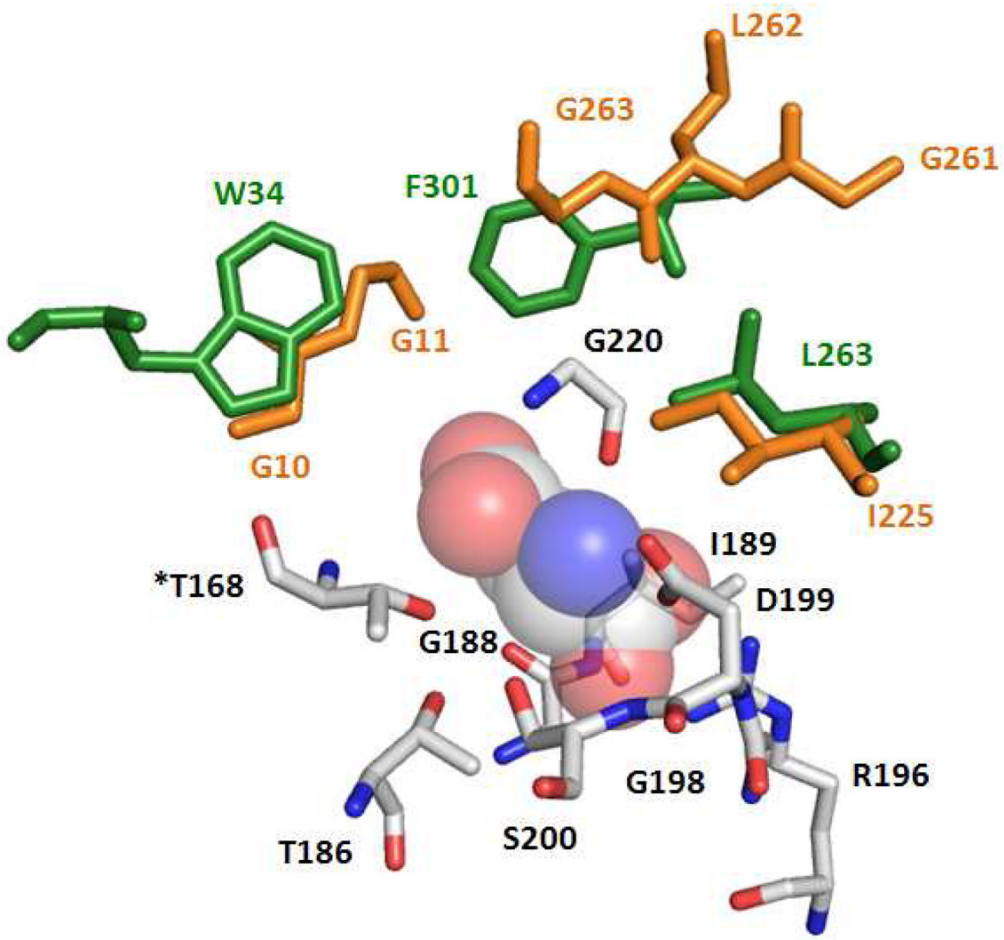

Fig 5.

Predicted human ASRGL1 (hASRGL1) active site overlaid against the human aspartylglucosaminidase (AGA) active site. A model of hASRGL1 structure based on *E. coli* isoaspartyl aminopeptidase/L-asparaginase (EcAIII) was obtained from Phyre (*33*) [Job code: 45ae21e95bf1f71f, SCOP code c2zakA, E-value 7.5e-41, Identity 35%, Estimated precision 100%] and aligned to human AGA (PDB: 1APZ; with bound L-aspartate) using PyMol (*34*). Bound L-aspartate is shown as spheres. Amino acids conserved between the two structures are colored by CPK and are numbered by hASRGL1 sequence (asterisk indicates the nucleophilic Thr). Amino acids shaded green are specific to human AGA and those shaded orange are specific to hASRGL1. For additional detail, please refer to the “Discussion” section.

Table 1

Summary of kinetic parameters for hASRGL1-catalyzed hydrolysis of various substrates. Reactions were all carried out at 37°C, pH 7.4. n.d. = not within detection limit.

Substrate	K_{cat}(s^{-1})	K_M (mM)	K_{cat}/K_M($mM^{-1}s^{-1}$)
L-Asp β-methyl ester	7.7 ± 0.3	0.4 ± 0.004	21 ± 1.0
β-L-Asp-L-Phe	3.0 ± 0.1	0.4 ± 0.04	8 ± 1.3
β-L-Asp-L-Ala	6.0 ± 0.2	1.0 ± 0.1	6 ± 0.8
β-L-Asp-L-Leu	5.0 ± 0.2	1.2 ± 0.1	4 ± 0.5
L-Asn	6.9 ± 0.2	3.4 ± 0.3	2 ± 0.3
β-L-Asp-L-Phe methyl ester	3.5 ± 0.1	1.6 ± 0.2	2 ± 0.3
β-L-Asp-L-Lys	5.3 ± 0.4	5.2 ± 1.2	1 ± 0.3
GlcNAc-L-Asn	-	n. d.	-
L-Gln	-	n. d.	-